PHYSICAL REVIEW D VOLUME 49, NUMBER 6 15 MARCH 1994

Penrose's quasilocal mass in a numerically computed space-time

D. H. Bernstein*
National Center for Supercomputing Applications, 605 East Springfield Avenue, Champaign, Illinois 61820

K. P. Tod
Mathematical Institute and St John's College, Oxford, OX1 3LB, United Kingdom
(Received 13 September 1993)

We describe a numerical calculation of Penrose's quasilocal mass on a sequence of axisymmetric two-surfaces in the three-surface of time symmetry of a numerically constructed vacuum space-time corresponding to a Brill gravitational wave interacting with a Schwarzschild black hole. The resulting mass is positive, responds very sensitively to the presence of gravitational waves, and tends rapidly to the ADM mass outside the wave. The isoperimetric inequality for black holes and the hoop conjecture of Thorne are investigated with this definition of mass.

PACS number(s): 04.25.Dm, 04.20.Ex

I. INTRODUCTION

In any numerical calculation of the evolution of an isolated system in general relativity an important issue is always the radiation of energy out of the system to infinity. To give meaning to these terms, it is helpful to have a definition of the mass of the system "close in" to be compared with one of the standard definitions of mass asymptotically and thereby detect the radiation.

In many specific calculations, *ad hoc* definitions of mass can be found which work well enough. They are typically coordinate dependent, which may not be a problem when the coordinates are uniquely determined by the geometry of the problem. However, it would be desirable, for logical simplicity if for no other reason, to have a single uniform definition of mass close in which could be used in all circumstances and which was manifestly invariant. Penrose's "quasilocal mass" [1] was intended to provide just such a uniform definition: the aim of the quasilocal mass construction as originally given was to measure the total mass, momentum, and angular momentum, gravitational as well as material, threading through an arbitrary, topologically spherical, spacelike two-surface S in an arbitrary space-time M. The construction is quasilocal in the sense of being determined solely by the the metric and connection of M at S.

Subsequent study has shown that the original aim of Penrose's construction cannot be achieved with the construction in its original form. However, for a large class of surfaces S, the "noncontorted" ones in the language of Sec. II, it is possible to define a total mass within S. Furthermore, the results obtained for noncontorted surfaces are encouraging, and show that many distinct kinds of mass energy, including radiating gravitational energy, are successfully captured by the Penrose definition. (For a review of the construction, its successes with noncontorted S and its difficulties with contorted S see [2].)

In this paper we present a calculation of Penrose's quasilocal mass for a class of axisymmetric two-surfaces S in a class of axisymmetric space-times, the "black hole plus Brill wave" space-times of Sec. III. We believe this to be the first published example of a numerical study of the quasilocal mass construction, although an unpublished study of the mass of the static, axisymmetric Weyl solutions was made by Jeffryes [3].

The Penrose construction calls first for the solution of a system of elliptic equations on the surface S, followed by integration over S of a functional of the solutions. While this can be difficult analytically, it fits naturally into a program of numerically calculating space-times. Our aim has been partly to show how to implement the calculation practically, but also to study the results as providing a further test of the "reasonableness" of the Penrose definition of mass. In this context, one looks for positivity of the mass (which is not a foregone conclusion), for a correlation with one's intuition about processes which increase or decrease mass, for a suitable approach to the known asymptotic limits and for consistency with what has been called the "isoperimetric inequality for black holes."

The isoperimetric inequality for black holes [4,5] is the inequality

$$16\pi(\text{mass})^2 \geq \text{area} \tag{1}$$

which is conjectured to apply to black holes. When the mass is defined asymptotically, then (1) is a prediction of the cosmic censorship hypothesis. For a static black hole, and with the mass being the Penrose mass, (1) can be reduced to an inequality for functions on the sphere, and then proved [2]. Although one does not have the compelling reason provided by the Cosmic Censorship Hypothesis for believing (1) quasilocally, nonetheless it is an interesting question to test it, not just for black holes, but also for marginally trapped surfaces.

Another inequality, similar in some respects to the isoperimetric inequality for black holes, is the hoop inequality for black holes conjecture by Thorne [6]. This

*Present address: Department of Mathematics, Statistics, and Computing Science, University of New England, Armidale, NSW 2351, Australia.

inequality is

$$4\pi(\text{mass}) \geq \text{circumference of horizon.} \tag{2}$$

While "area" in (1) is uniquely defined, "circumference" in (2) is not obvious. However, for axisymmetric surfaces there are clear notions of equatorial and polar circumference which, in a certain sense, are the most "reasonable" definitions of circumference [7]. Hence one can test (2) with the quasilocal mass and axisymmetric marginally trapped surfaces.

The plan of this paper is as follows.

In Sec. II, we review the quasilocal mass construction of Penrose and indicate how it associates a mass to a noncontorted two-surface S.

In Sec. III, we review the numerical construction of axisymmetric initial data for the "black hole plus Brill wave" space-time. The data depend on a choice of one free function $q(\eta, \theta)$ and we make a particular choice of a three-parameter family of functions for q.

In Sec. IV, we show how to adapt the general scheme of Sec. II to the specific metric of Sec. III. We present an algorithm for calculating the quasilocal mass at a surface S by first solving a coupled system of ordinary differential equations (ODE's), then performing integrations of functionals of the solutions of this system to define a 2×2 matrix, and finally taking the determinant of this matrix.

The results are presented in Sec. V. We consider how the geometry of the initial surface changes with the three parameters in q, and how these changes are reflected in variations in the mass. We note the asymptotic behavior of the mass, and comment on the tests provided by the isoperimetric inequality (1) and the hoop inequality (2). There is a brief summary and conclusion in Sec. VI.

II. PENROSE'S QUASILOCAL MASS CONSTRUCTION

In 1982, Penrose proposed a construction [1] with the ambitious aim of associating a momentum and angular momentum to an arbitrary, spacelike, topologically, spherical two-surface S in an arbitrary spacetime. The construction was intended to measure the total momentum and angular momentum, gravitational as well as material, threading through S. Most subsequent investigations of the construction, and most of the success achieved, has involved the more modest aim of defining a total mass, in the sense of the length of the momentum vector, for any S.

For brevity, we will use the term *kinematical quantities* for the total momentum together with the total angular momentum. The construction begins by considering the definition of the kinematical quantities for an isolated system, first in special relativity and then in linearized general relativity.

In special relativity, for each Killing vector k^a in Minkowski space, one obtains a conserved current $T_{ab}k^b$ from the stress-tensor T_{ab} of the isolated system. Integration of this current over a spacelike three-surface yields one of the kinematic quantities of the source: a component of momentum if the Killing vector is translational and a component of angular momentum if the Killing vector is a rotation.

In linearized general relativity, the kinematical quantities of the source can be measured in the external gravitational field which the source produces. Mathematically, this is because the three-surface integral can be turned into a two-surface integral over a two-surface outside the source, in the external field. The two-surface integrand is a product of the linearized curvature with a spinorial quantity which is a potential for a Killing vector. There is a 10-dimensional vector space V of these potentials, and the ten kinematical quantities are thereby unified into a single object, an element of the dual of V.

The flat-space construction is carried over to curved space as follows: given the two-surface S, first find a way to identify the vector space V of these potentials; then use them with the full curvature tensor to form the same integrand; this will give a definition of the ten, linearly independent kinematical quantities in curved space. (See [8] or [9] for this material and the quasilocal mass construction; see [2] for a review of the quasilocal mass construction.)

To be more concrete, we need some notation. A spacelike two-surface S has a pair of null directions normal to it at each point. These define a normalized spinor dyad (o^A, ι^A: $o_A\iota^A = 1$) at each point. The vector space V is obtained from the *two-surface twistor space* $\mathbf{T}(S)$ of S which, in turn, is the four-dimensional complex vector space of spinor fields ω^A on S which satisfy the *two-surface twistor equations*:

$$o_A\delta\omega^A = 0, \qquad \iota_A\bar{\delta}\omega^A = 0\ , \tag{3}$$

where $\delta = o^A\bar{\iota}^{A'}\nabla_{AA'}$ (we will be using the Newman-Penrose spin-coefficient formalism freely; see, e.g., Newman and Penrose [10], Penrose and Rindler [8]).

Equation (3) defines an elliptic system on spinor fields ω^A. The index (in the sense of the Atiyah-Singer index theorem) of the operator is 4, so that on a generic S the space of solutions $\mathbf{T}(S)$ is four dimensional. The two-surface twistor equations are motivated by twistor theory in Minkowski space, and from that theory we know that the vector space V of potentials for Killing vectors is the symmetric tensor product $\mathbf{T}(S) \odot \mathbf{T}(S)$. If $\{\omega_i{}^A : i = 1,2,3,4\}$ are the spinor fields defining a basis $\{Z_i\}$ of $\mathbf{T}(S)$, then a basis of V is represented by the (ten linearly independent) symmetric, valence-2 spinor fields $\{\omega_i{}^{(A}\omega_j{}^{B)}\}$.

With respect to the bases just introduced, the kinematic quantities for a vacuum space-time are defined by the following integral over S:

$$A_{ij} = -\frac{i}{4\pi}\int_S \Psi_{ABCD}\,\omega_i{}^A\,\omega_j{}^B\,d\sigma^{CD}\ , \tag{4}$$

where Ψ_{ABCD} is the Weyl spinor and we have chosen units so that Newton's constant G is equal to one. In the presence of matter the integrand in (4) has another term involving the Ricci tensor.

The 4×4 symmetric matrix $A = (A_{ij})$ apparently has ten complex components. However, in linearized gravity it has a Hermiticity property which reduces it to ten real components, the correct number for the four components of momentum and six components of angular momentum.

In a general curved space-time and with a general S it is not known how to define and establish the appropriate generalization of this Hermiticity property, and this is a problem for the Penrose construction.

It is at this point, therefore, that one chooses a more modest course and seeks to construct a single scalar from A to represent total mass. In flat-space twistor theory, $\mathbf{T}(S)$ comes equipped with a pseudo-Hermitian inner product Σ. This inner product can be used to define the norm of A, and in flat-space twistor theory this norm defines the total mass in the sense of the Minkowski, metric length of the total momentum vector, P^a:

$$m^2 = g_{ab}P^aP^b = -\frac{1}{2}\Sigma(A, A). \tag{5}$$

Since the inner product is indefinite, there is no guarantee *a priori* that the quantity on the right in (5) will be positive. However, for sources in linearized general relativity satisfying an energy condition, it can be shown that the momentum defined in this way is indeed time-like and future pointing.

To be able to use (5) we need to have Σ available. Associated with any element of $\mathbf{T}(S)$, or equivalently with any spinor field ω^A on S satisfying (3), there is another spinor field $\pi_{A'}$ on S defined by

$$\pi_{A'} = \pi_{1'}\bar{o}_{A'} - \pi_{0'}\bar{\iota}_{A'} ,$$

$$\pi_{1'} = -i\,\iota_A\delta\omega^A, \quad \pi_{0'} = i\,o_A\bar{\delta}\omega^A. \tag{6}$$

In flat space twistor theory, the spinor $\pi_{A'}$ is automatically covariant constant (this cannot happen in curved space, of course). Further, the inner product Σ on $\mathbf{T}(S)$ is defined with the aid of the $\pi_{A'}$ as follows: given a pair of elements Z_i, Z_j of the basis $\{Z_i\}$ of $\mathbf{T}(S)$, take the corresponding spinor fields $\omega_i{}^A$, $\omega_j{}^A$ and their associated $\pi^i{}_{A'}$, $\pi^j{}_{A'}$; now construct the quantity

$$\Sigma_{i\bar{j}} = \omega^A{}_i\bar{\pi}^j{}_A + \pi^i{}_{A'}\bar{\omega}^{A'}{}_j \tag{7}$$

then $\Sigma_{i\bar{j}}$, although built from spinor fields which vary on S, is actually constant on S, i.e., (7) defines a number and this number is the inner product $\Sigma(Z_i, Z_j)$.

In curved space, one may define $\pi_{A'}$ from ω^A as in (6) and then seek to define the inner product Σ by (7). However, for a generic S the quantity defined by (7) will not be constant on S and so will not serve to define an inner product on $\mathbf{T}(S)$. Without the inner product one cannot define the total mass as in (5). How should one proceed?

One course is to look for other definitions of norm; another is to restrict to two-surfaces S on which (7) does define a norm. Penrose [11] has suggested that surfaces S for which (7) is constant for every i and j should be called *noncontorted* and other surfaces *contorted*. It can be shown that a surface is contorted if it can "detect" through its first and second fundamental forms that it is in the presence of conformal (Weyl) curvature: a surface is noncontorted if it can be embedded in a conformally flat space-time with the same first and second fundamental forms [12, 13].

Although they are nongeneric, it is possible to find large classes of noncontorted two-surfaces in different space-times and calculate a quasilocal mass for each of them according to (5). By and large the results are quite satisfactory [2]. One result worth noting here is that, while the construction is tailored to give the right answer in the limit of general relativity which is linearized general relativity, it also turns out to give the right answer in the other limit which is Newtonian and post-Newtonian gravity [14].

It is also worth comparing the Penrose defintion with the Hawking definition of mass [15]: both definitions are genuinely *quasilocal* on a two-surface S in the sense that they depend only on the first and second fundamental forms of S (that is, on the space-time metric and space-time Christoffel symbols just at S); however the Penrose definition will always give zero for an S in flat space, while the Hawking definition will not in general; further, for a sequence of two-surfaces contracting onto a disc or onto a rod, like confocal spheroids in flat space, the Penrose mass will tend to zero even in curved space, while the Hawking mass will diverge to infinity even in flat space.

To connect with the work described in this paper, we note that, if a space-time has a hypersurface-orthogonal rotation Killing vector then any axisymmetric two-surface is automatically noncontorted [3,16]. The metrics of Sec. III have such a symmetry; thus the quasilocal mass of axisymmetric surfaces in these metrics can be defined.

To finish this section, we record another expression for A. This can be obtained from (4) by integration by parts using the definition (6) of the $\pi_{A'}$ field associated with an ω^A field and is

$$A_{ij} = -\frac{i}{4\pi}\int \pi^i{}_{A'}\,\pi^j{}_{B'}\,d\sigma^{A'B'}. \tag{8}$$

In Sec. IV, the existence of two expressions for A will provide a check on numerical accuracy.

III. THE BLACK HOLE PLUS BRILL WAVE SPACE-TIME

The space-time we propose to study has been under investigation by the numerical relativity group at NCSA for the past several years. It consists of a single black hole interacting with an ensemble of gravitational radiation. The space-time contains a surface of time symmetry upon which the metric is given a form similar to that first studied by Brill [17] for self-interacting gravitational waves. In addition each spatial hypersurface is given $\mathbf{S}^2 \times \mathbf{R}$ topology, sometimes called the Einstein-Rosen bridge topology [18]. As in the Schwarzschild space-time, we may endow hypersurfaces with this topology with a metric which is reflection symmetric through a special two-surface. This surface is then a closed trapped surface [19] and so the space-times will generally contain black holes. Hence we call them "black hole plus Brill wave space-times." In this section we will briefly discuss the time symmetric slice only, for an overview of the entire space-time see [20–22].

We work in the 3+1 formalism in which space-time is viewed as a foliation of three dimensional hypersurfaces each with a positive definite metric. The Einstein equa-

tions are written in terms of the first and second fundamental forms of the hypersurfaces, γ_{ab} and K_{ab} (in this section only latin indices will be restricted to the range $\{1,2,3\}$). The ten equations naturally break into four elliptic constraint equations, which must be satisfied on each slice, and six hyperbolic evolution equations, which, when given the geometry of an initial slice, may be used to compute the geometry of subsequent slices. The contracted Bianchi identity guarantees that the evolution equations maintain the constraints as long as they are satisfied on an initial slice.

The initial value problem of general relativity then consists of finding a three-metric and extrinsic curvature which satisfy the Hamiltonian and momentum constraint equations

$$R + (\mathrm{tr}K)^2 - K^{ab}K_{ab} = 0, \tag{9}$$

$$D_b(K^{ab} - \gamma^{ab}\mathrm{tr}K) = 0\ , \tag{10}$$

where R is the scalar curvature and D_a the covariant derivative associated with γ_{ab}. These equations may be put into an essentially elliptic form by the well-known York conformal decomposition method [23]. In this method some components of γ_{ab} and K_{ab} are specified beforehand and the equations are then used to find the remaining components.

Here we will consider initial data on time symmetric hypersurfaces. Time symmetry requires the extrinsic curvature to vanish and so the momentum constraint is satisfied identically. The initial three-metric is given the form studied by Brill:

$$ds^2 = \Psi^4\left[e^{2q}\left(d\eta^2 + d\theta^2\right) + \sin^2\theta d\phi^2\right]. \tag{11}$$

Here η is a radial coordinate while θ and ϕ are the familiar spherical polar coordinates on the constant η two-spheres. The function q is arbitrary and one may use it to specify the form of the wave. The remaining degree of freedom in γ_{ab}, the conformal factor Ψ, is then determined by the Hamiltonian constraint.

Metric (11) is already in the conformal form $\gamma_{ab} = \Psi^4\hat{\gamma}_{ab}$ necessary for York's method. The conformal transformation of the scalar curvature is

$$R = \Psi^{-4}\hat{R} - 8\Psi^{-5}\hat{\Delta}\Psi, \tag{12}$$

and the Hamiltonian constraint becomes the linear equation

$$\hat{\Delta}\Psi = \frac{1}{8}\Psi\hat{R}, \tag{13}$$

where careted quantities are formed out of $\hat{\gamma}_{ab}$ in the usual way. Given the Brill wave form of the metric (11) this equation reduces to

$$\frac{\partial^2\Psi}{\partial\eta^2} + \frac{\partial^2\Psi}{\partial\theta^2} + \frac{\partial\Psi}{\partial\theta}\cot\theta = -\frac{1}{4}\Psi\left(\frac{\partial^2 q}{\partial\eta^2} + \frac{\partial^2 q}{\partial\theta^2} - 1\right). \tag{14}$$

In this work q is chosen to be in what we call an "inversion symmetric Gaussian" form

$$q = af(\theta)\left(\exp\left[-\left(\frac{\eta+b}{w}\right)^2\right] + \exp\left[-\left(\frac{\eta-b}{w}\right)^2\right]\right). \tag{15}$$

There are three independent parameters a, b, and w which, roughly speaking, specify the amplitude, range, and width of q, and an angular dependence given by $f(\theta)$. In this paper we will consider only initial data with $f = \sin^2\theta$. Thus our initial hypersurfaces are equatorial plane symmetric, in addition to being axisymmetric.

The Hamiltonian constraint (14) is an eigenvalue-like equation and may be solved using methods for elliptic equations. The numerical details of its solution may be found in [20, 21]. The numerical method was the following: the domain of computation is taken to be $0 \le \eta \le 6$ and $0 \le \theta \le \pi/2$ (in the Schwarzschild space-time $\eta = 0$ is the location of the event horizon and $\eta = 6$ lies at $202M$), the grid is set to be evenly spaced in both η and θ with $\Delta\theta$ as close as possible to $\Delta\eta$. Second-order centered finite difference approximations to the derivatives of Ψ are substituted into (14) resulting in an inhomogeneous set of linearly equations to be solved for the value of Ψ at each grid point (the Robin condition, see York [24], is used at the outer boundary). The linear equations are then solved as a matrix inversion problem. Various error quantities may be formed out of the solution and from these the rate of convergence of the solution was determined to be second order in the grid spacing. The data for this work was generated on a grid with 200 points in the radial direction and 53 points in the angular direction.

When the amplitude parameter a is set to zero we regain the Schwarzschild space-time. In this case the solution to the Hamiltonian constraint is

$$\Psi = \sqrt{2M}\cosh(\eta/2) \tag{16}$$

and the radial coordinate η is related to the Schwarzschild radial coordinate r by

$$r = \Psi^2 = 2M\cosh^2(\eta/2). \tag{17}$$

In these coordinates the initial three-metric takes the form

$$ds^2 = 4M^2\cosh^4(\eta/2)\left[d\eta^2 + d\theta^2 + \sin^2\theta d\phi^2\right]. \tag{18}$$

Note that $\eta \to -\eta$ is an isometry with $\eta = 0$ the isometry surface (i.e., the fixed points of the isometry, sometimes called the "throat" of the Einstein-Rosen bridge). The black hole plus Brill wave space-time is constructed such that this remains true on the time symmetric slice (and, incidentally, on every subsequent slice of the numerically generated spacetime).

The physical and geometrical properties of the initial surface as a function of the parameters a, b, and w are discussed in some detail in [20, 21]. Here we will only mention the properties of the apparent horizon as this has implications for the quasilocal mass. The method of Cook [25] was used to located the horizon (see also [26]). In the Schwarzschild space-time the apparent and event

horizons coincide and on the $t = 0$ slice the apparent horizon is located at $r = 2M$ or $\eta = 0$. For initial data sets with $b = 0$ and $w = 1$ the isometry surface remains the apparent horizon if $-0.65 < a < 3.03$. If a is less than -0.65 the apparent horizon occurs outside of the isometry surface. For data sets with $b > 0$ the horizon detaches from the throat at a higher absolute value of a: $a = -0.84$ for $b = 0.5$ and $a = -1.42$ for $b = 1$. Once the apparent horizon is found its proper area may be computed. The mass of the apparent horizon is defined to be proportional to the square root of its proper area:

$$m_{\mathrm{AH}} \equiv \sqrt{\frac{A}{16\pi}}. \tag{19}$$

The geometry of the horizon may be visualized by way of an embedding in a flat three-dimensional Euclidean space. Here a surface in the flat space is constructed so as to have the same metric as that intrinsic to the horizon. The method used to construct the embedding was somewhat nonstandard, however, comparison with the standard method gave the same result. In general the horizon has the geometry of a prolate two-sphere for $a > 0$ and that of an oblate 2–sphere for $a < 0$. Figure 1(a) shows cross sections of the embedding diagrams for the data sets $-0.144 \leq a \leq 1$, $b = 0$, and $w = 1$. When a is decreased below -0.144 the Gaussian curvature becomes negative on the axis and no (axisymmetric) embedding in a Euclidean space can be constructed.

Another measure of the shape of the horizon is obtained by computing the ratio of its polar and equatorial circumferences. For data sets with $b = 0$ and $w = 1$ this ratio is shown in Table I. The ratio may be very large; embeddings of the horizon for $a > 1$ are very long, thin spindles. Note also that an axisymmetric surface embedded in a Euclidean space has a *minimum* value of the ratio of circumferences. A very thin pancakelike figure with radius r will have polar circumference approximately $4r$ and equatorial circumference $2\pi r$; the ratio is $2/\pi$ or about 0.637. The ratio of circumferences of the surface $\eta = 0$ attains this figure at $a = -0.34$ and drops below it for a less than this value (note that the apparent horizon lies outside the throat for $a < -0.65$). That the initial slice permits such a surface is an indication of its deviation from both Euclidean geometry and the spherically symmetric geometry of the Schwarzschild initial slice.

In general, for $a > 0$ all of the constant η surfaces have the geometry of prolate two-spheres and for $a < 0$ that of oblate two-spheres. The maximum deviation from sphericity occurs when η is in the neighborhood of the range parameter b. An example is shown in Fig. 1(b) where the embeddings of a family of constant η surfaces for the data set $a = 1$, $b = 0$, $w = 1$ are plotted. The distortion is greatest at the throat where the wave is centered and quickly dies off as η is increased. By $\eta = 2.0$ the surfaces are essentially spherical.

IV. CALCULATING THE PENROSE MASS

In this section we show how the general theory of Sec. II can be used to calculate the quasilocal mass on a two-surface S of constant η in the metrics of Sec. III. The calculation begins by writing the relevant equations in the Newman-Penrose (NP)–formalism [10, 8].

First, we choose a null tetrad tailored to the geometry. In terms of the metric and coordinates of (11) define

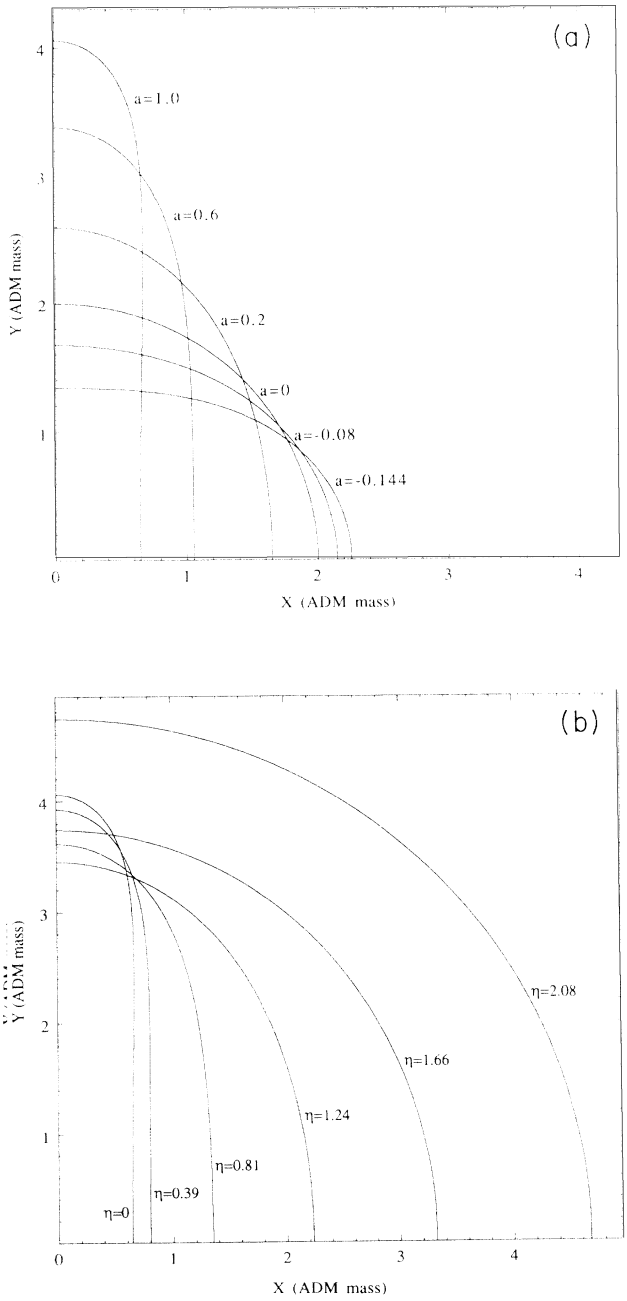

FIG. 1. (a) Embeddings of the throat as a function of the Brill wave amplitude a with $b = 0$ and $w = 1$. The flat space axes are in units of the ADM mass for each initial data set. (b) Embeddings of the constant η surfaces for initial data set $a = 1$, $b = 0$, and $w = 1$. The flat space axes are in units of the ADM mass.

TABLE I. Ratio of polar to equatorial circumference of the surface $\eta = 0$ as a function of the amplitude a with $b = 0$ and $w = 1$. Note that for $a = -1$ the throat is no longer the apparent horizon.

a	-1.0	-0.5	0.0	0.5	1.0	1.5	2.0	2.5	3.0
C_p/C_e	0.2803	0.5189	1.000	2.020	4.282	9.497	21.90	52.14	127.2

$$l = \frac{1}{\sqrt{2}}\left(T + \frac{1}{\Psi^2 e^q}\frac{\partial}{\partial\eta}\right),$$

$$n = \frac{1}{\sqrt{2}}\left(T - \frac{1}{\Psi^2 e^q}\frac{\partial}{\partial\eta}\right), \tag{20}$$

$$m = \frac{1}{\sqrt{2}\,\Psi^2}\left(\frac{1}{e^q}\frac{\partial}{\partial\theta} + \frac{i}{\sin\theta}\frac{\partial}{\partial\phi}\right),$$

where T is the unit normal to the intial hypersurface. Then l and n are the null normals to S, and m is the complex null tangent to S, with the imaginary part of m aligned with the Killing vector.

Next, we calculate the spin coefficients for this tetrad. The relevant spin coefficients for our calculation are α, β, λ, μ, σ, and ρ. To calculate them, we must use the fact that the tetrad given by (20) is on a surface of time symmetry, i.e., the second fundamental form is zero. We find

$$\alpha = -\beta = -\frac{1}{2\sqrt{2}\,\Psi^2 e^q}\left(\cot\theta + \frac{2}{\Psi}\frac{\partial\Psi}{\partial\theta}\right),$$

$$\sigma = \lambda = -\frac{1}{2\sqrt{2}\,\Psi^2 e^q}\frac{\partial q}{\partial\eta}, \tag{21}$$

$$\rho = \mu = -\frac{1}{2\sqrt{2}\,\Psi^2 e^q}\left(\frac{\partial q}{\partial\eta} + \frac{4}{\Psi}\frac{\partial\Psi}{\partial\eta}\right).$$

The symmetry makes these spin coefficients real and forces the other relations among them.

The null tetrad defines a normalized spinor dyad (o^A, ι^A) in the usual way and we expand ω^A and $\pi_{A'}$ in this dyad with the standard conventions:

$$\omega^A = \omega^0 o^A + \omega^1 \iota^A, \quad \pi_{A'} = \pi_{1'}\bar{o}_{A'} - \pi_{0'}\bar{\iota}_{A'}. \tag{22}$$

Now we can write out (3) in the NP formalism as

$$(\delta - \beta)\,\omega^1 - \sigma\omega^0 = 0\,, \quad (\bar{\delta} + \alpha)\,\omega^0 + \lambda\omega^1 = 0, \tag{23}$$

where

$$\delta = m^a\nabla_a = \frac{1}{\sqrt{2}\,\Psi^2}\left(\frac{1}{e^q}\frac{\partial}{\partial\theta} + \frac{i}{\sin\theta}\frac{\partial}{\partial\phi}\right) \tag{24}$$

while (6) becomes

$$\pi_{0'} = i\left[(\bar{\delta} - \alpha)\,\omega^1 - \rho\omega^0\right],$$

$$\pi_{1'} = i\left[(\delta + \beta)\,\omega^0 + \mu\omega^1\right]. \tag{25}$$

Inspection of the spin coefficients shows that Eqs. (23) have an extra symmetry: if (ω^0, ω^1) is a solution then so is $(\bar{\omega}^1, -\bar{\omega}^0)$. A convenient way to separate the ϕ dependence turns out to be

$$\omega^0 = \Psi\, G\, e^{i\phi/2}; \quad \omega^1 = \Psi\, F\, e^{i\phi/2}, \tag{26}$$

and then the system (23), with the spin coefficients given above, becomes

$$\frac{\partial F}{\partial\theta} - \frac{(e^q + \cos\theta)}{2\sin\theta}F = -\frac{1}{2}\frac{\partial q}{\partial\eta}G,$$

$$\frac{\partial G}{\partial\theta} + \frac{(e^q - \cos\theta)}{2\sin\theta}G = \frac{1}{2}\frac{\partial q}{\partial\eta}F. \tag{27}$$

We need two linearly independent solutions (F_1, G_1), (F_2, G_2) to (27) and by inspection of the Wronskian we may normalize them by

$$G_1F_2 - F_1G_2 = \frac{1}{2}\sin\theta. \tag{28}$$

Taking account of the extra symmetry noted above, we may write the general solution of (23) as

$$\omega^0 = \Psi\left[(a_1G_1 + a_2G_2)e^{i\phi/2} + (a_3F_1 + a_4F_2)e^{-i\phi/2}\right],$$

$$\omega^1 = \Psi\left[(a_1F_1 + a_2F_2)e^{i\phi/2} - (a_3G_1 + a_4G_2)e^{-i\phi/2}\right], \tag{29}$$

where a_i, $i = 1, 2, 3, 4$, are coordinates on $\mathbf{T}(S)$.

If we substitute (29) into (25), we find the corresponding associated general $\pi_{A'}$ field, and then we may substitute into (7) to find the inner product. The result of this last calculation, using the normalization (28), turns out to be

$$\Sigma_{ij}a_i\bar{a}_j = \omega^A\bar{\pi}_A + \bar{\omega}^{A'}\pi_{A'} = \frac{-i}{\sqrt{2}}(a_1\bar{a}_2 - a_2\bar{a}_1 + a_4\bar{a}_3 - a_3\bar{a}_4). \tag{30}$$

As anticipated, all dependence on θ and ϕ has disappeared from (30) because S is noncontorted.

At this point we have the two-surface twistors explicitly and we have the inner product. The next step is to calculate A, either using (4) and (29) or using (8) and (25). This leads to

$$A = -iA_{ij}a_ia_j = -\frac{i}{4\pi}\int \Psi_{ABCD}\,\omega^A\,\omega^B\,d\sigma^{CD} \tag{31}$$

[here, for later convenience, we have introduced a factor $(-i)$. Thus A_{ij} from (31) differs by this factor from A_{ij} in Sec. II]. In the first case we find

$$A_{13} = \int_0^\pi \left[V(F_1^2 - G_1^2) + 2UF_1G_1\right] \Psi^2 e^{-q} \sin\theta d\theta \,,$$

$$A_{24} = \int_0^\pi \left[V(F_2^2 - G_2^2) + 2UF_2G_2\right] \Psi^2 e^{-q} \sin\theta d\theta \,,$$

$$A_{14} = A_{23} = \int_0^\pi \left[V(F_1F_2 - G_1G_2) + U(F_1G_2 + F_2G_1)\right] \Psi^2 e^{-q} \sin\theta d\theta \,, \tag{32}$$

and all other components of A are zero, where

$$U \equiv \frac{1}{\Psi}\frac{\partial^2\Psi}{\partial\eta\partial\theta} - \frac{3}{\Psi^2}\frac{\partial\Psi}{\partial\eta}\frac{\partial\Psi}{\partial\theta} - \frac{1}{\Psi}\frac{\partial q}{\partial\theta}\frac{\partial\Psi}{\partial\eta} - \frac{1}{\Psi}\frac{\partial q}{\partial\eta}\frac{\partial\Psi}{\partial\theta} - \frac{1}{2}\frac{\partial q}{\partial\eta}\cot\theta, \tag{33}$$

$$V \equiv -\frac{1}{2} + \frac{1}{\Psi}\frac{\partial^2\Psi}{\partial\theta^2} - \left(\frac{1}{\Psi}\frac{\partial\Psi}{\partial\theta}\right)^2 + \frac{1}{\Psi}\frac{\partial\Psi}{\partial\theta}\cot\theta - \frac{1}{2}\frac{\partial q}{\partial\theta}\cot\theta - \frac{1}{\Psi}\frac{\partial q}{\partial\theta}\frac{\partial\Psi}{\partial\theta} + 2\left(\frac{1}{\Psi}\frac{\partial\Psi}{\partial\eta}\right)^2 + \frac{1}{\Psi}\frac{\partial q}{\partial\eta}\frac{\partial\Psi}{\partial\eta}, \tag{34}$$

while in the second case

$$A_{13} = -\frac{1}{2}\int_0^\pi \left[\left(XF_1 + \frac{2}{\Psi}\frac{\partial\Psi}{\partial\eta}G_1\right)^2 - \left(YG_1 - \frac{2}{\Psi}\frac{\partial\Psi}{\partial\eta}F_1\right)^2\right] \Psi^2 e^{-q}\sin\theta\, d\theta,$$

$$A_{24} = -\frac{1}{2}\int_0^\pi \left[\left(XF_2 + \frac{2}{\Psi}\frac{\partial\Psi}{\partial\eta}G_2\right)^2 - \left(YG_2 - \frac{2}{\Psi}\frac{\partial\Psi}{\partial\eta}F_2\right)^2\right] \Psi^2 e^{-q}\sin\theta\, d\theta, \tag{35}$$

$$A_{14} = A_{23} = -\frac{1}{2}\int_0^\pi \left[\left(XF_1 + \frac{2}{\Psi}\frac{\partial\Psi}{\partial\eta}G_1\right)\left(XF_1 + \frac{2}{\Psi}\frac{\partial\Psi}{\partial\eta}G_1\right) - \left(YG_1 - \frac{2}{\Psi}\frac{\partial\Psi}{\partial\eta}F_1\right)\left(YG_2 - \frac{2}{\Psi}\frac{\partial\Psi}{\partial\eta}F_2\right)\right] \Psi^2 e^{-q}\sin\theta\, d\theta,$$

and all other components of A are zero, where

$$X = \frac{\cos\theta + e^q}{\sin\theta} + \frac{2}{\Psi}\frac{\partial\Psi}{\partial\theta},$$

$$Y = \frac{\cos\theta - e^q}{\sin\theta} + \frac{2}{\Psi}\frac{\partial\Psi}{\partial\theta}. \tag{36}$$

Again we emphasize that (32) and (35) are simply related by integration by parts but it is useful for computational purposes to have two different expressions. The quantities U and V are closely related to Weyl tensor components at S. It is a simple matter to calculate from these the curvature quantities which go into the integral (4) for A_{ij}. In terms of U and V these are

$$\Psi_1 = -\Psi_3 = \Psi^{-4}e^{-2q}U, \quad \Psi_2 = \Psi^{-4}e^{-2q}V. \tag{37}$$

For vanishing q, i.e., spherical symmetry, equations (27) decouple and the solutions are easily seen to be

$$F = a\sin(\theta/2), \quad G = b\cos(\theta/2); \quad \text{constant } a,\ b. \tag{38}$$

If we introduce f and g by

$$(F, G) = (f\sin(\theta/2), g\cos(\theta/2)) \tag{39}$$

then (27) becomes

$$\frac{\partial f}{\partial\theta} + \frac{f(1-e^q)}{2\sin\theta} = -\frac{g}{2}\frac{\partial q}{\partial\eta}\cot(\theta/2),$$

$$\frac{\partial g}{\partial\theta} - \frac{g(1-e^q)}{2\sin\theta} = \frac{f}{2}\frac{\partial q}{\partial\eta}\tan(\theta/2), \tag{40}$$

and the normalization condition becomes

$$g_1f_2 - g_2f_1 = 1. \tag{41}$$

f and g must satisfy the boundary conditions

$$\left.\frac{\partial f}{\partial\theta}\right|_{\theta=0} = \left.\frac{\partial f}{\partial\theta}\right|_{\theta=\pi} = \left.\frac{\partial g}{\partial\theta}\right|_{\theta=0} = \left.\frac{\partial g}{\partial\theta}\right|_{\theta=\pi} = 0. \tag{42}$$

If the two-surface happens to be equatorial plane symmetric, as in our space-times, we may generate another solution from a given solution (F_1, G_1) by

$$(F_2(\pi-\theta), G_2(\pi-\theta)) = (G_1(\theta), F_1(\theta)) \,, \tag{43}$$

or

$$(f_2(\pi-\theta), g_2(\pi-\theta)) = (g_1(\theta), f_1(\theta)) \,. \tag{44}$$

Finally, to obtain the quasilocal mass we must calculate the norm of A given by (32) or (35) using the inner product implicitly defined by (30). This gives

$$m^2 = -A_{13}A_{24} + A_{14}A_{23}. \tag{45}$$

The numerical calculation proceeds as follows.

(1) We choose the Brill wave parameters a, b, and w and solve the Hamiltonian constraint for the conformal factor Ψ.

(2) The two-surface twistor equations (40) are solved with the initial conditions $f = 1$ and $g = 0$ at $\theta = 0$. Another set is generated by the symmetry relation (44) and these are normalized according to (41). An implicit Adam's method in the package ODEPACK was used to perform the integration. Note that no interpolation is needed because all of the quantities appearing in (40) are given exactly in terms of θ. The maximum allowable residual of the equations is set at 3×10^{-3} (F, G, f, and g are all dimensionless) and fourth-order centered finite difference approximations are used in the equations to generate the residuals. The normalization condition (41) is checked and the solution is rejected if there is a maximum deviation greater than 1×10^{-4}. The fully "dressed" two-surface twistors (F, G) are then constructed and the solutions to (27) and the normalization condition (28) are checked according to the same tolerances.

(3) The kinematic twistor is constructed using both (32) and (35). The Penrose mass is constructed from both expressions and the two are compared. The solution is rejected if the percentage difference is greater than 1×10^{-4}.

(4) If the solution is rejected at any step then different sets of initial conditions are tried whereby $g(0) = 0$ and $f(0)$ ranges from 0 to 2. However, except in extreme cases, adequate solutions were usually found with $f(0) = 1$.

A tentative check of the accuracy of the calculation may be made by comparing the result with the Arnowitt-Deser-Misner (ADM) mass when the two are computed on the outermost $\eta =$ constant shell. When this is done, by computing the Penrose mass with the above procedure, the relative difference between the Penrose mass and the ADM mass is on the order of 10^{-6} if the range parameter b is less than 2 and the amplitude is not too large ($-1 \leq a \leq 2$). This difference rises rapidly when the range is greater than 2 to about 10^{-2} at $b = 3$ (this is evident in Fig. 3).

In the figures in the following section we will plot the quasilocal mass as a function of η and the Brill wave parameters a, b, and w. With these fixed we may ask how quickly the Penrose mass converges to a set value as the grid is refined so as to get an idea of how large the "error bars" should be around the points on these figures. In Table II we show the convergence of the mass in two typical cases, one low amplitude and one high amplitude. We see that the mass varies by no more than five parts in 10^5 when the resolution is quadrupled from 200 radial by 53 angular points, the value at which the data displayed in this paper was computed, to 400×105 points.

TABLE II. Convergence of the Penrose mass taken at $\eta = 0$ for representative initial data sets: $a = 1$, $b = 0$, $w = 1$, and the same with $a = 0.1$. m_0 is a preset scale parameter, constant for all initial data sets, which in the Schwarzschild space-time is equal to the mass of the hole. (The ADM mass itself generally varies with the Brill wave parameters and hence also with the resolution.) The grid size is the number of points in the η direction $\times$ the number of points in the θ direction. The outermost point is located at $\eta = 6$ in each case.

	$a = 1$		$a = 0.1$	
Grid size	m (m_0)	m (ADM)	m (m_0)	m (ADM)
100×27	42.93177	38.90189	0.984806	1.034517
200×53	42.89451	38.89884	0.984786	1.034629
300×79	42.88744	38.89833	0.984781	1.034665
400×105	42.88495	38.89698	0.984782	1.034678

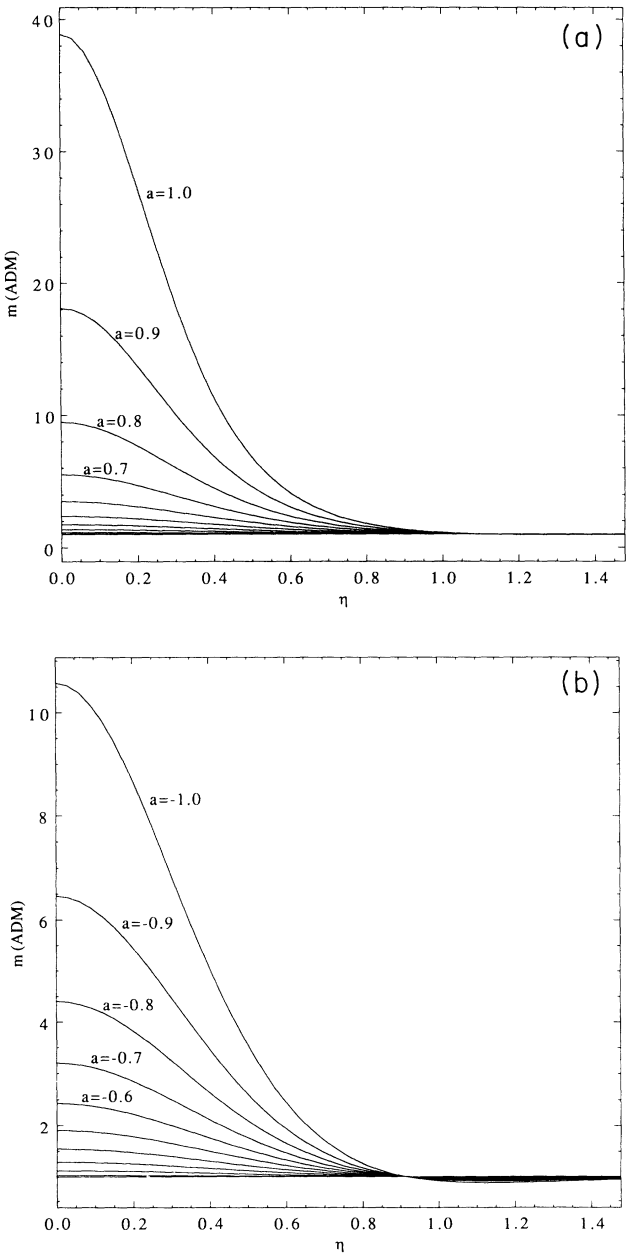

FIG. 2. (a) The Penrose mass taken on the constant η surfaces for data sets $0 \leq a \leq 1$ with $b = 0$ and $w = 1$. The data is in units of $m_{\rm ADM}$. (b) The Penrose mass on the constant η surfaces for data sets $-1 \leq a \leq 0$ with $b = 0$ and $w = 1$. The data is in units of $m_{\rm ADM}$.

V. EXAMPLES

In this section we present in graphical form the results of calculating the quasilocal mass of Sec. IV in the spacetimes of Sec. III. In Figs. 2 and 3 we plot the quasilocal mass m of Eq. (45), in units of the ADM mass $m_{\rm ADM}$ to which it tends at infinity, against the radial coordinate η. The scale starts at $\eta = 0$ which is the minimal surface at the throat.

In Fig. 2 the parameters b and w of Eq. (15), which determine the location and width of the Brill wave part of the data, are taken to be 0 and 1, respectively: the wave is centered at the throat. In Fig. 2(a) the mass is plotted against η for a range of positive values of the amplitude a, and in Fig. 2(b) for a range of negative values of a. Recall from Fig. 1 that an increase in a in the positive direction corresponds to an increasingly prolate throat, and an increase in a in the negative direction corresponds to an increasingly oblate throat.

From Fig. 2 we see that m rises rapidly as compared to $m_{\rm ADM}$ with increasing deformation of the throat, much more rapidly than, for example, a geometric measure of the deformation like the ratio of polar and equatorial circumferences. Also, the rate of rise with $|a|$ is greater toward a prolate deformation. [Something similar to this is seen in the quasilocal mass of comoving cylinders in the locally rotationally symmetric (LRS) cosmologies, where the quasilocal mass rises rapidly with the length of the cylinder and diverges much more rapidly than the shear on the approach to the singularity [27, 28].]

The quasilocal mass drops rapidly with increasing distance to the asymptotic value, $m_{\rm ADM}$. Recall that the gravitational disturbance at the horizon has width parameter one and, by $\eta = 1$, m is very close to $m_{\rm ADM}$. In Fig. 2(b), m actually overshoots $m_{\rm ADM}$ but it returns to approach it from above. In other cases, m may oscillate several times about $m_{\rm ADM}$.

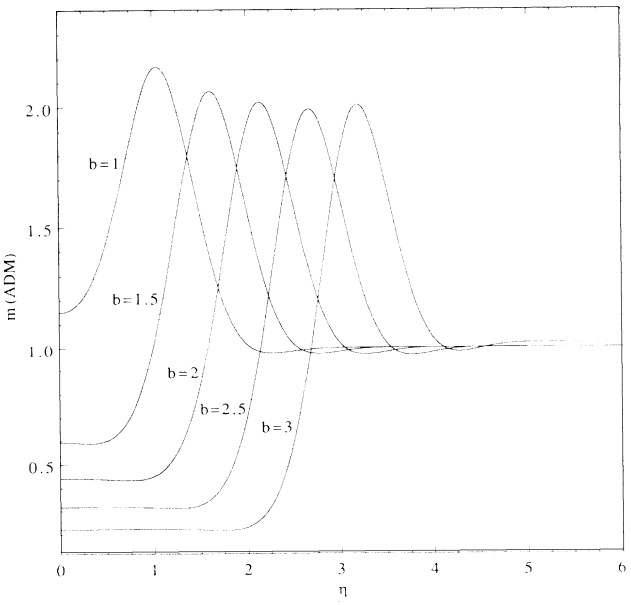

FIG. 3. The Penrose mass on the constant η surfaces for data sets $1 \leq b \leq 3$ with $a = 1$ and $w = 1$. The data is in units of $m_{\rm ADM}$.

In Fig. 3, m is plotted against η for a variety of values of the parameter b with $a = 1$ and $w = 1$. Varying b corresponds to varying the location of the Brill wave, and in Fig. 3 we see that m rises from its value at the throat to a maximum at the location of the wave before dropping back to its asymptotic value. This location also corresponds to the location of extrema of various measures of the curvature, e.g., the curvature invariants $R_{abcd}R^{abcd}$ and $R^{ab}{}_{cd}R^{cd}{}_{ef}R^{ef}{}_{ab}$, the Weyl tensor component Ψ_4 (37), and the York curvature tensor components. Note that m at the throat may be greater or less than $m_{\rm ADM}$.

What we see from these figures is that m is real and nonzero, which there was no guarantee of from its defining equation (45), m responds very sensitively to gravitational waves distorting the Schwarzschild background, and, from Fig. 3, peaks at the location of the waves, m tends to $m_{\rm ADM}$ asymptotically, as one knows from general theory; the fact that m reaches $m_{\rm ADM}$ so rapidly outside the wave is an indication that the data rapidly approach the data for Schwarzschild, since m is known to be equal to $m_{\rm ADM}$ for any topologically spherical surface in a constant-time hypersurface in the Schwarzschild solution [13], and m is very definitely not monotonically increasing with increasing radius.

This last point calls for comment. Since the quasilocal mass *is* quasilocal, it is not the integral over a spanning three-surface of a local density. Indeed, for the situation considered here with the Einstein-Rosen bridge topology, there are no spanning three-surfaces. Correspondingly, there is no 'flux-formula' for the difference in quasilocal mass between neighboring concentric two-surfaces: if one moves the two-surface out to a larger radius, one must simply calculate m again on the new two-surface. The expression (45) for m in terms of A_{ij} is quadratic, so even in a situation where the A_{ij}'s for different surfaces are additive, as for example in the time-symmetric-initial-value-problem [29], the masses will not be. From this last example, one knows that the quasilocal mass detects gravitational potential energy, which is negative in as much as it reduces total mass. If the mass drops with increasing radius, that does not mean that there is a patch of "negative-energy-density", rather it means that the total energy within the two-surface, *including gravitational potential energy*, has decreased.

The remaining figures are related to the isoperimetric inequality and the hoop inequality discussed in the Introduction. Again, our motivation is twofold, both to investigate these inequalities and to provide support for the quasilocal mass definition.

Figure 4 shows m on the throat in units of $m_{\rm AH}$, the irreducible mass of Eq. (19). Inequality (1) is the requirement that this ratio be greater than one. In Fig. 4(a), the ratio is plotted for $b = 0$, $w = 1$ and a in the range $-0.5 < a < 0.5$ and in Fig. 4(b) on a different vertical scale with $0 < a < 1$. For this range of parameters, there is no other minimal surface outside the throat, i.e., the throat is the apparent horizon.

The ratio has a very attractive minimum at unity when

$a = 0$, which is the Schwarzschild solution, and then m increases rapidly away from m_{AH} as the deformation increases. In the discussion of Fig. 2 we noted that m increases rapidly as compared with one geometric measure of deformation, the ratio of circumferences; here we see it increasing rapidly as compared with another, the square root of the area.

In Fig. 4(c) the same ratio is plotted with $b = 2$ and $w = 1$ with the range $-1.6 < a < 3$. Again, there is a minimum of the ratio at the Schwarzschild solution and otherwise it is greater than one, increasing in both directions with increasing deformation. Both the isoperimetric inequality and the quasilocal mass survive this encounter.

Figure 5 shows a "hoop-ratio" $4\pi m/C$ at the throat $\eta = 0$ plotted against a for the data set with $b = 0$ and $w = 1$ which was used in Figs. 4(a) and 4(b) (and also in Figs. 1 and 2). The circumference C is taken to be the larger of the polar and equatorial circumferences. The two branches of the curve are for the two different circumferences, which are equal for the Schwarzschild solution at $a = 0$ where the two branches meet.

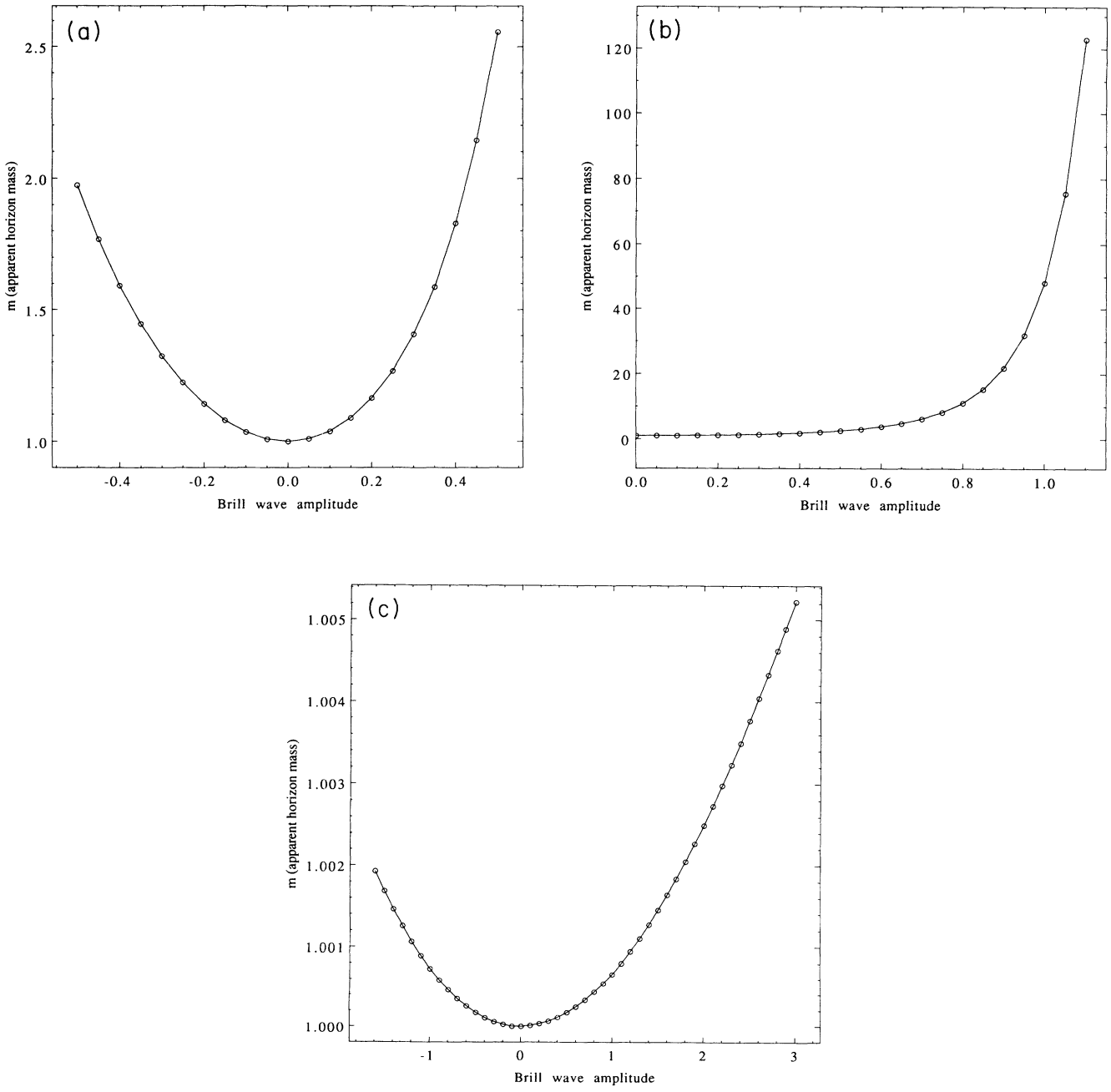

FIG. 4. An investigation of the isoperimetric inequality. The Penrose mass is taken on the apparent horizon ($\eta = 0$ in all cases) for the data sets: (a) $-0.5 \leq a \leq 0.5$ with $b = 0$ and $w = 1$. (b) $0 \leq a \leq 1.1$ with $b = 0$ and $w = 1$. (c) $-1.6 \leq a \leq 3$ with $b = 2$ and $w = 1$. m is in units of m_{AH} in each figure.

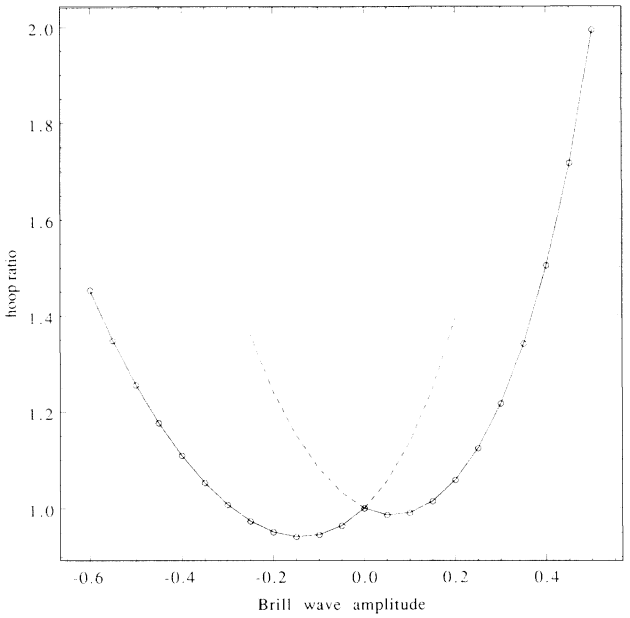

FIG. 5. An investigation of the hoop inequality. We show the "hoop ratio" $4\pi m/C$ taken on the apparent horizon ($\eta = 0$) as a function of the Brill wave amplitude a for data sets $-0.6 \leq a \leq 0.5$ with $b = 0$ and $w = 1$. The circumference C is taken to be the larger of the polar and equatorial circumferences of the apparent horizon.

In both directions, the hoop ratio, which should be greater than one for a literal interpretation of (2), drops below one away from Schwarzschild, so the result is less clear-cut than for the isoperimetric inequality. Still there are minima on both branches of the curve so that an inequality such as (2) but with a number slightly greater than 4π on the left-hand side will hold. Graphs similar to Fig. 5 may be drawn for other data sets, and lead to similar conclusions. Other studies of the hoop conjecture have also indicated that a different number might be needed [30, 31] and Thorne [6] never claimed that "4π" was cast in stone. With these qualifications, we have found some support for the "only if" part of the hoop conjecture ["black holes form only if (2) holds"].

We noted above that the Penrose mass m decreases with radius at least for some coordinate ranges. There is an interesting vindication of this property in connection with the hoop inequality. If one uses the ADM mass instead of the Penrose mass to test the hoop inequality one will not in general find that the inequality is satisfied. For example, for the data set $a = 1$, $b = 0$, $w = 1$, the ratio $4\pi C/m_{\mathrm{ADM}}$ is 0.72, and for $a = 2$ and $a = 3$ it is 0.41 and 0.15, respectively (for $a = -0.6$ it is 0.60). Hence the ratio is a decreasing function of a when computed with the ADM mass and an increasing function when computed with the Penrose mass. This implies that any definition of mass which increases monotonically with the radial coordinate η and approaches the ADM mass at infinity could only satisfy the hoop inequality (taken on the apparent horizon) with a number on the left hand side greater than 4π by a rather large factor, at least six or seven on the evidence of this particular family of initial data sets.

VI. SUMMARY AND CONCLUSIONS

We have shown that it is a practical matter to calculate Penrose's quasilocal mass numerically for axisymmetric two-surfaces as part of the process of numerically constructing an axisymmetric space-time. It is important for the calculation that such two-surfaces are guaranteed to be noncontorted, but the mass so obtained then has reasonable properties. It is nonzero, it responds sensitively to gravitational radiation, peaking where, intuitively, we would expect the radiation to be, and it rapidly approaches the ADM mass at large distances.

The calculation of the mass is moderately laborious as compared with other, more *ad hoc* definitions, but the definition has the virtue of having a solid rationale, and being universally applicable, at least on noncontorted two-surfaces. When used as a test of the isoperimetric and hoop inequalities, the quasilocal mass provides satisfactory answers which reinforce both the status of the inequalities and the use of this definition of mass in them.

It remains to be studied how the quasilocal mass will fare in a numerical calculation of a dynamical space-time. The principle of the calculation would remain the same, at least for an axisymmetric space-time, but the calculation would be more complex in detail. From the study of cylindrical gravitational waves, which can be handled explicitly, one knows that the quasilocal mass will rise and fall in time with the passage of the wave.

ACKNOWLEDGMENTS

D.B. would like to thank William Shaw for a useful conversation and the members of the relativity group at NCSA for their support. This research was supported in part by the National Center for Supercomputing Applications.

[1] R. Penrose, Proc. R. Soc. London **A381**, 53 (1982).
[2] K.P. Tod, in *Twistors in Mathematics and Physics*, edited by T.N. Bailey and R.J. Baston, LMS Lecture Note Series Vol. 156 (Cambridge University Press, Cambridge, England, 1990).
[3] B.P. Jeffryes, report, 1986 (unpublished).
[4] R. Penrose, Ann. N.Y. Acad. Sci. **224**, 125 (1973).
[5] G.W. Gibbons, in *Global Riemannian Geometry*, edited by T. Willmore and N.J. Hutchins (Ellis Horwood, New York, 1984).
[6] K.S. Thorne, in *Magic Without Magic*, edited by J. Klauder (Freeman, San Francisco, 1972).

[7] E. Flanagan, Phys. Rev. D **44**, 2409 (1991).
[8] R. Penrose and W. Rindler, *Spinors and Space-Time* (Cambridge University Press, Cambridge, England, 1986), Vols. 1 and 2.
[9] S.A. Huggett and K.P. Tod, *An Introduction to Twistor Theory* (Cambridge University Press, Cambridge, England, 1985).
[10] E.T. Newman and R. Penrose, J. Math. Phys. **3**, 896 (1962).
[11] R. Penrose, Twistor Newsletter **18** (1984).
[12] B.P. Jeffryes, in *Asymptotic Behaviour of Mass and Space-Time*, edited by F.J. Flaherty, Springer Lecture Notes in Physics (Springer, Berlin, 1984).
[13] K.P. Tod, Class. Quantum Grav. **3**, 1169 (1986).
[14] B.P. Jeffryes, Class. Quantum Grav. **3**, 841 (1986a).
[15] S.W. Hawking, J. Math. Phys. **9**, 598 (1968).
[16] B.P. Jeffryes, Proc. R. Soc. London **A411**, 59 (1987).
[17] D.S. Brill, Ann. Phys. (N.Y.) **7**, 466 (1959).
[18] A. Einstein and N. Rosen, Phys. Rev. **48**, 73 (1935).
[19] G.W. Gibbons, Commun. Math. Phys. **27**, 87 (1972).
[20] D.H. Bernstein, Ph.D. thesis, University of Illinois at Urbana-Champaign, 1993.
[21] D.H. Bernstein, D.W. Hobill, E. Seidel, P. Anninos, J. Towns, and L. Smarr (unpublished).
[22] A.M. Abrahams, D. Bernstein, D. Hobill, E. Seidel, and L. Smarr, Phys. Rev. D **45**, 3544 (1992).
[23] J.W. York, in *Sources of Gravitational Radiation*, edited by L.L. Smarr (Cambridge University Press, Cambridge, England, 1979).
[24] J.W. York, in *Frontiers in Numerical Relativity*, edited by C.R. Evans, L.S. Finn, and D.W. Hobill (Cambridge University Press, Cambridge, England, 1989).
[25] G.B. Cook, Ph.D. thesis, University of North Carolina at Chapel Hill, 1990.
[26] G.B. Cook and J.W. York, Phys. Rev. D **41**, 1077 (1990).
[27] K.P. Tod, Class. Quantum Grav. **4**, 1457 (1987).
[28] K.P. Tod, Class. Quantum Grav. **7**, 2237 (1990).
[29] K.P. Tod, Proc. R. Soc. London **A388**, 457 (1983).
[30] K.P. Tod, Class. Quantum Grav. **9**, 1581 (1992).
[31] C. Barrabès, W. Israel, and P. Letelier, Phys. Lett. A **160**, 41 (1991).